ELEKTROTEHNIŠKI VESTNIK 86(1-2): 29-36, 2019
ORIGINAL SCIENTIFIC PAPER

Design of a Six-Slot High-Speed Permanent-Magnet Generator with the Stator Core made of an Amorphous Magnetic Material

Flyur R. Ismagilov [1], Jing Ou [2], Viacheslav Ye. Vavilov [1], Denis V. Gusakov [1], Valentina V. Ayguzina [1*], Aleksey M. Veselov[1]

[1] *Department of Electromechanics, Ufa State Aviation Technical University, Russia*
[2] *Karlsruhe Institute of Technology, Germany*
**E-mail: vtipy@mail,ru*

Abstract. The paper describes a high-speed permanent-magnet generator with a power rating of 3–5 kW and a rotational speed of 48,000–96,000 rpm for powering unmanned aerial vehicles. Development trends in the magnetic core made of an amorphous magnetic material and possible topologies for its implementation are presented. Various generator topologies utilizing a newly implemented six-slot stator core made of an amorphous magnetic material are studied using a computer simulation. The new stator-core design is used and its effectiveness is experimentally proven. The manufacturing technology of the magnetic core made according to the proposed structure is described. A comparison is made between the losses in machines with the magnetic core made of an amorphous magnetic material and those in machines with the magnetic core made of electrical steel. Based on results of a computer simulation and experimental study, the most effective machine topology is determined and its superior efficiency due to using an amorphous magnetic material is proven.

Keywords: Amorphous Magnetic Materials, Magnetic Losses, Permanent-Magnet Machines

Zasnova generatorja s trajnimi magneti za visoke hitrosti vrtenja s šestimi utori in amorfnim statorskim feromagnetnim jedrom

V prispevku so predstavljeni generatorji s trajnimi magneti z močjo 3–5 kW in hitrostjo vrtenja 48,000–96,000 vrt./min. za napajanje brezpilotnih letalnikov. Predstavili smo trende na področju amorfnih magnetnih materialov in možnosti za njihovo uporabo v električnih strojih. Z računalniškimi simulacijami smo analizirali različne topologije generatorjev s šestimi utori in amorfnim statorskim feromagnetnim jedrom. Opisali smo zasnovo statorja in eksperimentalno preverili njegovo učinkovitost. Predstavili smo tudi tehnologijo izdelave predlaganega magnetnega jedra. Primerjali smo izgube glede na konvencionalne generatorje ter na podlagi računalniških simulacij in eksperimentov določili najučinkovitejšo topologijo in potrdili uporabnost amorfnega magnetnega materiala.

1 INTRODUCTION

High-speed permanent-magnet generators (HSPMGs) with a power-rating of 3–5 kW and rotational speed of 48,000–96,000 rpm are effectively used in various industries. They are used in small-sized micro-turbine installations for powering unmanned aerial vehicles (UAVs), satellites and in electro-mechanical energy-storage facilities [1]–[5]. Their wide application results from deployment as high-speed drive whose shaft is connected to the HSPMG rotor without a gearbox. This ensures a maximum reliability, since the absence of a gearbox and coupling contributes to a minimum overall dimension of the entire system, maximum efficiency and a maximum HSPMG power-to-mass ratio. For UAVs, the drive is a shaft of a turbojet engine with a rated power of up to 5 kW and a rotational speed of 60000–120,000 rpm [3]. The HSPMG application areas show a significant economic growth and have great perspectives for development, both economically and technically [6]. This sets the task of an increased efficiency for high-speed HSPMGs while minimizing their mass and overall dimension, along with reducing their prime cost.

A lot of effort has been devoted to increase the HSPMG energy efficiency while reducing its cost. The HSPMG loss-minimization issues are studied in [1]–[12], and the HSPMG losses remain one of the main limitations that significantly affect the HSPMG design and creation. Almost all projects [2], [4], [5], [10], [11] consider a two-pole HSPMG, since at high rotational speeds, an increase in the number of poles leads to an increase in the magnetization reversal frequency of the stator and, consequently, to an incommensurate increase in the eddy-current and hysteresis losses in the stator core. Calculations show that implementation of a 3–5 kW HSPMG with four to eight poles enables achievement of an HSPMG power-to-mass ratio of 5.5–6.7 kW/kg at a rotational speed of 48,000–96,000 rpm. This value

Received 5 December 2018
Accepted 12 February 2019

cannot be achieved for the two-pole HSPMG. Therefore, loss minimization in the stator core will not only increase the HSPMG efficiency, but also its power-to-mass ratio.

One way to minimize the losses in the stator core is to use an amorphous magnetic material (AMM). AMM is used mainly in a slotless HSPMG with a rated power of up to 100 W and a rotational speed above 100,000–150,000 rpm [13]–[14]. A slotless HSPMG has a low power-to-mass ratio and, therefore, does not effectively solve the HSPMG problems for UAV or spacecraft in the 3–5 kW power range. The efficiency of a 200–250 kW slotless HSPMG is proven in [15], but this case is an exception. A number of projects [16]–[17] present the AMM core for the axial-flux HSPMG, but the maximum rotational speed is limited by the rotor mechanical stress, and this falls below 30,000–40,000 rpm at a power above 7 kW. A study of a radial-flux HSPMG design with an AMM stator core is presented in [18]. Currently, there are no industrial designs that can find a wide application for UAV.

The main contribution of this paper is a comprehensive HSPMG AMM efficiency assessment, a technological research inability the use of AMM in HSPMG, and the design of several experimental 5-kW 60,000-rpm HSPMG prototypes by using this technology. In future, the study results will open up new opportunities for increasing the HSPMG efficiency by using AMM.

2 HSPMG TOPOLOGIES

The analyze [1]–[12] show that losses in the stator winding and core for a two-pole HSPMG with a 3–5 kW power-rating, 48,000–96,000 rpm rotational speed, distributed windings and ball bearings are practically the same; they vary from 20 to 25 % of the total losses [3], [7]. The considerable end winding length is a disadvantage of an HSPMG with a distributed winding. To resolve this problem, a tooth-coil winding is used. The eddy-current losses in PM and rotor sleeve can reach 17 % [15]. The PM eddy-current losses are lower than those in the stator winding and core. Nevertheless, they are difficult to be kept away from a fast-rotating rotor. These losses overheat PMs and lead to their demagnetization [9]. In various works [4], [7], [8] and [11], much attention is paid to have this loss type analyzed.

A new technology for the AMM-core manufacture is developed. The HSPMG stator core is designed with several separate cores made of an AMM tape (Fig. 1) wound onto a cylindrical drum. The number of cores corresponds to the number of the stator slots. To ensure an optimal use of the material, the cores have a triangular shape. The AMM cylindrical coils are installed on a technological mandrel with triangular notches and are impregnated. After that, the triangular

a) b)

Figure 1. AMM core created by the proposed technology (a) and triangular cores in the technological mandrel (b)

cores are subjected to a joint impregnation and glueing, and thus a stator of a necessary mechanical strength and magnetic properties is formed. To create open slots, a part of the AMM core is cut by using an abrasive wheel causing a slight deterioration of the AMM properties. To reduce the eddy-current and hysteresis losses, the stator core is formed of stacks less than 5 mm long and isolated from each other. To minimize the costs, the number of the slots should be minimal. Therefore, the most effective number of the slots of an HSPMG with an AMM stator core is either 3 or 6. A large number of the slots is technologically difficult to achieve, especially when the stator outer diameter is below 50 mm, which is the core with the prefabricated AMM stator core, and each tooth is created separately. An increase in the number of the slots will lead to an increase in the number of the stator-core sectors making their dimensions be insignificant. This will greatly complicate the stator-core assembly. Therefore, a limited number of topologies should be implemented. Fig. 2 shows the main topologies of the AMM stator core with six teeth and two or four poles.

In this paper, an experimental prototype of each of the HSPMG topologies (Fig. 2) with an AMM stator core is created and experimental results for each of them are described. HSPMG is intended for the use in the UAV power supply systems. It is considered a topology with a combined star delta winding and the studies of which are not given in known publications. The most effective HSPMG topology with an AMM stator core is selected. The results show the possibility of a widespread practical use of HSPMG for UAV.

In our case, a topology with a 5BDSR grade of AMM, 1.35 T saturation magnetic-flux density and the tape thickness of 25 μm is studied. This grade is similar to Metglas 2605 in terms of the physical and chemical properties. The stator consists of nine 5 mm long stacks. The total stator length is 45 mm. The Sm_2Co_{17} permanent magnets with a residual magnetic-flux density of 1.07 T and a magnetic field strength of 756 kA/m are used in the rotor magnetic system. To minimize the losses, PMs are laminated in the axial direction. The rotor active length is 50 mm and it consists of five 10 mm long magnets. A carbon fiber sleeve is installed over the magnets. The winding wire is of the “PNET-imid” type with a temperature index of

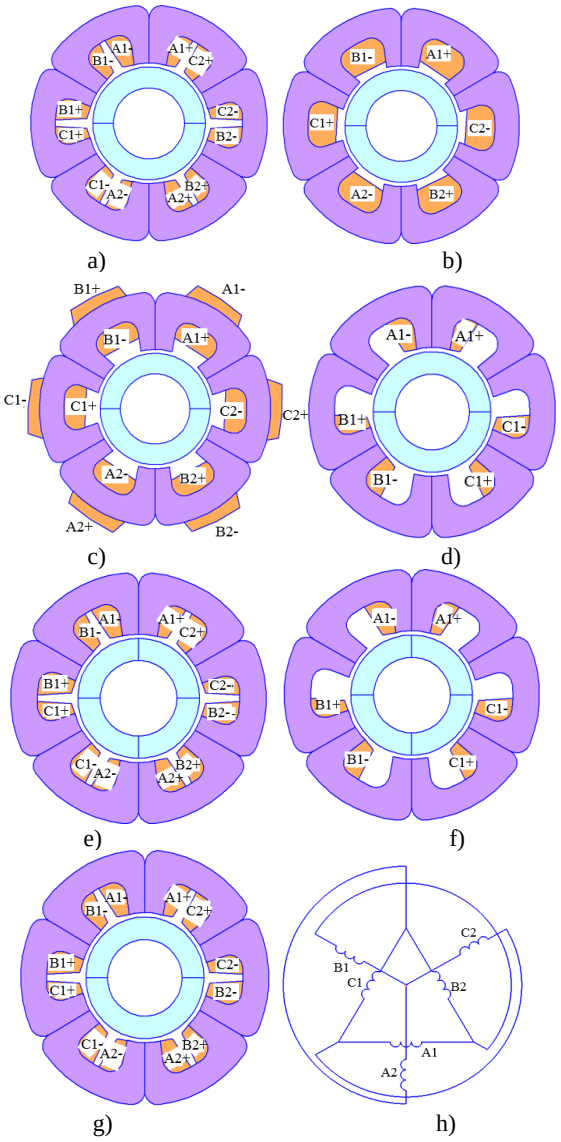

Figure 2. HSPMG topologies: a) Type-A with a tooth-coil winding; b) Type-B with a distributed winding; c) Type-C with a toroidal winding; d) Type-D with a tooth-coil winding; e) Type-E with a tooth-coil winding; f) Type-F with a tooth-coil winding; g) Type-G with a combined star delta winding; h) combined star delta winding scheme.

220 °C. The slot is insulated with a polyamide film. The wire diameter is selected as follows. The depth of the magnetic-field penetration into the wire is calculated. The wire diameter is less than this depth making the eddy currents to be resistance-limited [19]. To simplify the layout manufacture, the wire diameter in of each prototype is the same, so the magnetic-field penetration depth is calculated for the highest frequency for each topology (60,000 rpm, four poles, 2000 Hz). Therefore, a two-strand wire of a 0.8 mm diameter is used for each layout. Table 1 show parameters of the studied topologies. For each of them, the stator core is the same, and only the number of the turns and the winding type vary. Fig. 3 shows the stator and rotor dimensions for each topology. The SKF 638/8-2Z [20] bearings providing a speed of up to 90,000 rpm are used.

Table 1. Parameters of studied topologies

Topology	**A**	**B**	**C**	**D**	**E**	**F**	**G**
Power, kW				5			
Number of rotor poles	2	2	2	2	4	4	2
Number of stator slots				6			
Rated current, A				14.49			
Rotational speed, rpm				60,000			
RMS phase voltage, V				115			
Turn number in phase	20	10	10	20	8	8	20
Total stator core length with end windings, mm	58	80	55	68	54	60	58
Active stator length, mm				45			
Outer stator diameter, mm				68			
HSPMG outer diameter with housing, mm	73	73	78	73	73	73	73
PM diameter, mm				28			
Rotor sleeve diameter, mm				31			
Air gap, mm				1			
Stator material	5BDSR grade of AMM with a 1.35 T saturation magnetic flux density						
PM type	Sm_2Co_{17}, B_r = 1.07 T, H_c = 756 kA/m						
Sleeve material, mm	Carbon fiber with a 2 mm thickness						
Winding factor	0.5	1	1	0.5	0.9	0.87	0.5
Active resistance, μΩ	38	25	38	35	21	21	38
Cooling	Forced air						

The topologies are selected according to the following criteria:

– Steepness of the volt-ampere characteristic showing the HSPMG overload capability. Its requirements are set in the MIL STD 704 standard.

– Maximum-fault tolerance. The value of the short-circuit current should be minimal to ensure a safe HSPMG operation. The HSPMG winding should not be interconnected.

– Minimal harmonic distortion of the output voltage.

– Maximum efficiency to minimize the requirements for the cooling system and the volume of the pumped refrigerant as specified on the UAV board.

– Maximum power-to-mass ratio since UAV has a limited capacity and HSPMG should occupy a minimum space on the UAV board.

The Type-A topology is a well-known topology with a tooth-coil winding. The low 0.5 winding factor reduces the topology efficiency. This topology has large PM eddy-current losses due to the MMF spatial harmonics.

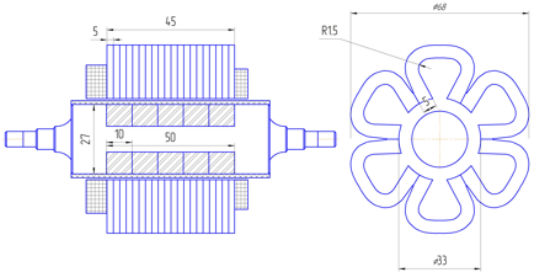

Figure 3. HSPMG dimensions

Because of the simplicity of its implementation and the minimum end-winding axial protrusion length is used in a HSPMG with a power rating of 3–5 kW and a rotational speed of 48,000 rpm or more. It is suitable for a two-pole rotor magnetic system, as well as for a four-pole rotor magnetic system of the Type-E topology. Due to the eddy-current and hysteresis losses in the stator core, the number of poles is usually minimal. As the losses in the stator core are reduced by using AMM, a four-pole rotor magnetic system is used without a significant loss increase, but with a significant increase in the power-to-mass ratio due to the increased voltage frequency with a constant rotational speed. The winding factor of the Type-E topology is 70 % higher than if the two-pole topology. Efficiency evaluation of the Type-A and Type-E topology used in the new stator design with AMM is not given in the literature.

The Type-B topology is also a well-known topology of the distributed windings. In contrast to the Type-A topology, this topology ensures minimum PM eddy-current losses. At the same time, the overall dimension is large due to the considerable end-winding axial protrusion length which increases the HSPMG size and decreases the critical rotational speed. HSPMG is usually operated near its rotational speed limit thus making every millimeter of its length crucial. Therefore, this winding type is rarely used in HSPMG.

The Type-C topology is a special case of the Type-B topology with a toroidal winding. The end winding and axial HSPMG dimensions are thus minimal. Compared to other topologies, the stator diameter is bigger because of the winding located on the outer stator surface. A disadvantage of this topology are higher phase resistance and copper losses for not using the outer winding. The outer winding can be used for HSPMG heat removal and gradient cooling. In general, it is used in a slotless HSPMG [13], [14].

The Type-D and Type-F topology are a two-pole and four-pole variety of the Type-A and Type-E topology. In these topologies, one winding occupies only one slot. It increases the HSPMG fault tolerance due to a smaller mutual inductance.

The Type-G topology is of interest for having a combined star-delta winding with a tooth-coil design and because these are only studies of a combined winding for the induction motors and not for the synchronous electric machines, in particular not for HSPMGs.

3 Computer Simulations

Experimental results do not allow analyzing all HSPMG processes as it is particularly difficult to experimentally determine the eddy-current losses in PM and to estimate the total HSPMG magnetic-field distribution. For a thorough analysis of the HSPMG effectiveness, this data is mandatory. Therefore, computer models of each topology are analyzed and verified against the experimental results.

The first step is a computer simulation using the Ansys Maxwell software package. The PM eddy-current losses and the magnetic-flux density distribution in the stator core are estimated, and a conclusion is drawn about the effectiveness of individual HSPMG topologies. Fig. 4 shows the magnetic-flux density distribution in a no-load mode for the Type-A and Type-E topology. The magnetic-flux density in the teeth of a four-pole topology is lower than in a two-pole topology by 18–20 %. This reduces the core mass or minimizes the losses without changing the overall dimension. The losses in the stator core can be estimated using the known expression [21]:

$$P_{\mathrm{c}} = k_{\mathrm{h}} B^2 f + k_{\mathrm{c}} B^2 f^2 + k_{\mathrm{ex}} (Bf)^{3/2} \qquad (1)$$

where $k_{\mathrm{h}}, k_{\mathrm{c}}, k_{\mathrm{ex}}$ are the size coefficients of the hysteresis, eddy-current and excessive eddy-current losses, respectively, B is the magnetic-flux density, and f is the magnetization-reversal frequency.

To determine the coefficients, a preliminary loss measurement is taken in two AMM annular cores using a laboratory measurement device. One of the measured annular core is made of a 5BDSR integral tape of 50 mm of the axial length, while the other is made of ten glued cores, each of 5 mm of the axial length. The measuring winding is wound on both cores. At a 2000 Hz frequency and 1 T magnetic-flux density, the hysteresis and eddy-current losses in the stator core made of a 5BDSR integral tape are 28–30 W/kg, and in the core made of the ten glued cores, they are only 8 W/kg.

Taking into account the AMM loss approximation and the stator core made of 5 mm long stacks, the 5BDSR loss coefficients are as follows:

$$P_{\mathrm{c}} = 1.63 \cdot 10^{-3} B^2 f + 0.63 \cdot 10^{-6} B^2 f^2 + 0.54 \cdot 10^{-4} (Bf)^{3/2} \qquad (2)$$

By decreasing the magnetic-flux density and increasing

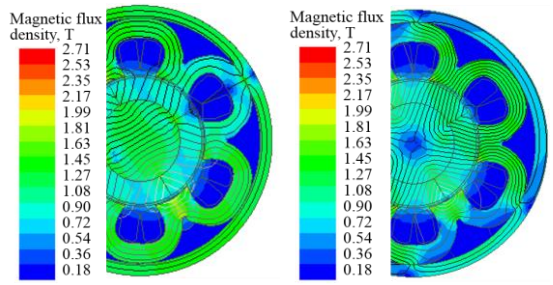

a) b)

Figure 4. Magnetic fields in HSPMG at a no-load mode: a) Type-A topology; b) Type-E topology

the number of poles from two to four at a constant rotational speed, the AMM losses increase by 90 %. The copper losses decrease by 89 % due to a smaller number of the turns of the four-pole topology with an increase in the stator current frequency. This proves that a four-pole topology with AMM can be very effective and not inferior in terms of the efficiency to two-pole topology. This conclusion differs from [10], where it is recommended to use a two-pole topology.

Fig. 5 shows the PM eddy-current losses for the studied topologies at a rotational speed of 60,000 rpm. The maximum eddy-current losses of the Type-E topology are approximately 38 W. In the Type-F topology, the losses are 23.8 W. This is only 1–1.5 W more than for the Type-A topology. This result proves that the Type-F topology efficiency is not lower than that of the Type-A topology. The fault tolerance and the power-to-mass ratio of the Type-F topology is higher than of the Type-A topology. The magnetization reversal frequency of the Type-F topology is 100 % higher than that of the Type-A topology. The Type-E and Type-F topology are very similar. The PM eddy-current losses in the Type-E topology are higher.

As the end windings of the Type-C topology are commensurable with the tooth-coil topology, this topology is maximally effective. It is inferior in terms of losses, although the winding resistance of the Type-C topology is higher than that of the Type-B topology. The PM eddy-current losses in the Type-G topology are 25 % smaller than in the Type-A topology, although the Type-G topology is also a two-pole HSPMG with a tooth-coil winding. Thus, in the first approximation, the Type-C and Type-F topology are the most effective. They enable a minimal axial dimension and maximal efficiency.

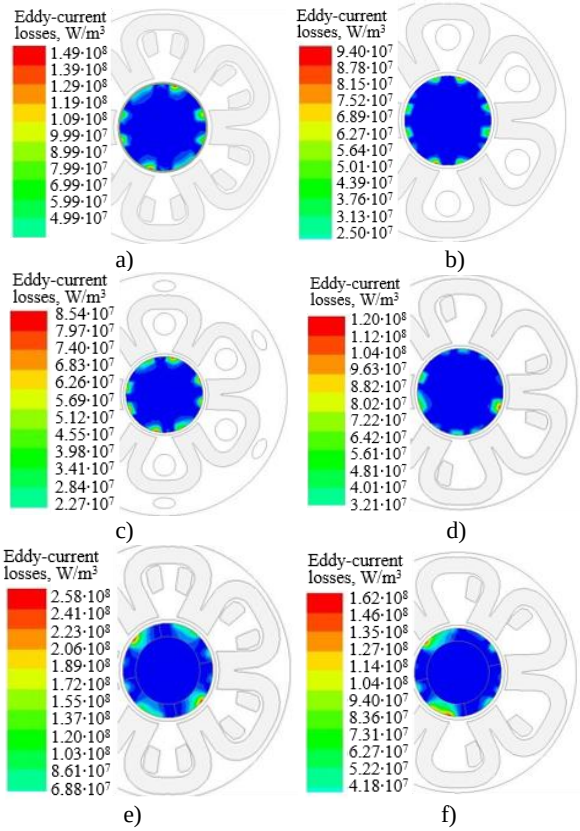

Figure 5. Losses in PM of the studied topologies: a) Type-A; b) Type-B; c) Type-C; d) Type-D; e) Type-F; f) Type-G

4 EXPERIMENTAL HSPMG STUDY

Eight full-size prototypes for each of the considered topologies are created. The experimental study is divided into two parts: 1) loss determination in the stator core made of AMM and FeSi on a special test bench; 2) efficiency evaluation of the HSPMG samples.

The operation principle of the test bench is based on the magnetization reversal of the ring sample made of a soft magnetic material on which the measuring and power winding are located. The magnetization reversal is performed by a dynamic hysteresis loop a 50-2000 Hz frequency. The power-winding voltage is assumed to be set. The magnetic hysteresis loops are recorded and the specific losses are determined. The specific-loss determination is based on measuring the active power consumed for the magnetization reversal, measuring devices (wattmeters and voltmeters), and amplifier feedback circuit. The voltage of the sample winding determines the active power indirectly. The RMS value of the magnetic-field strength is determined by measuring a magnetizing current measurement.

Specific losses are calculated as follows:

$$P_s = (1/m)\cdot\left(w_1 P_m / w_2 - U_1^2 / r_e\right)\cdot(1 + r_2 / r_e) \quad (3)$$

where m is the sample mass, w_1 and w_2 are the number of the turns of the power (magnetizing) and measuring winding, respectively, P_m is the average value of the active power, U_1 is the RMS voltage, r_2 is the total resistance of the measuring winding, r_e is the equivalent resistance of instruments and devices connected to the measured sample.

Using this method, the measurement error below 2.5 %. The drawback is that the magnetization reversal is carried out by a sinusoidal magnetic field. Therefore, all the cores are collected in HSPMG and the losses are directly measured following the measurements at the test bench. Fig. 6 shows the two-pole rotors and cores of the Type-A, Type-B, Type-C, Type-D topology. The magnetic cores of the Type-E, Type-F and Type-G topology are not given, as outwardly they do not differ from the Type-A and Type-D topology. Each topology is in the same housing and bearing shield. To compare the losses in a magnetic core made of AMM and FeSi, the Type-A topology is created with a FeSi stator core

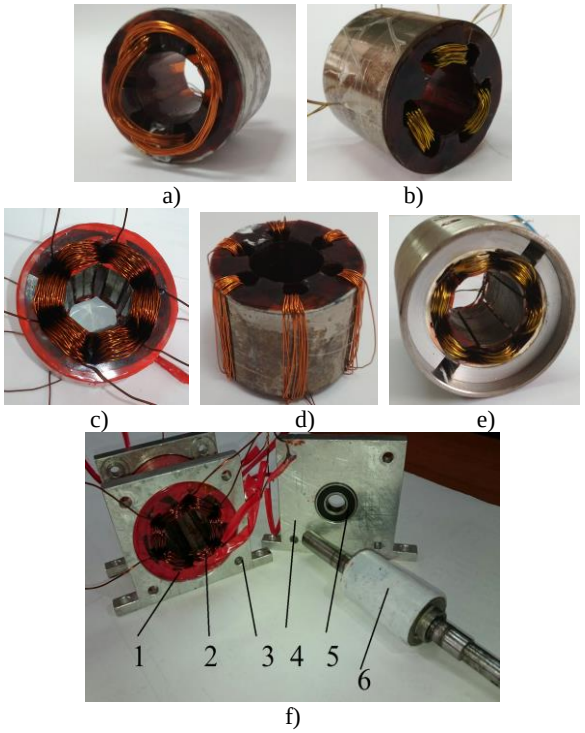

Figure 6. Experimental prototypes of HSPMG: a) B topology; b) D topology; c) A topology with an AMM core; d) C topology; e) A topology with an FeSi core; f) general setup of all topologies; 1 – stator; 2 – winding; 3 – housing; 4 – bearing shield; 5 – bearings; 6 – rotor.

(Fig. 6, e). Its prototype is tested on a stand (Fig. 7) at a low speed in the generator mode. To evaluate the AMM effectiveness, the HSPMG with FeSi is directly measured by estimating the power consumed by the drive (induction motor) and the output power of the sample. The HSPMG loss-estimation method is described below.

The tests are taken at a 60,000-rpm rotational speed and power rated below 1 kW due to the limitation set on the maximum power of the drive motor (1.2-kW 60,000-rpm). To evaluate the windage and friction losses, the two rotors are made of the same materials and with the same surface treatment. One rotor is made with PM, the other without it. The energy consumption of the drive motor is estimated by using a power analyzer. Initially, the losses are measured at the drive-motor start-up with a coupling and with no connection to HSPMG. The power consumption is 150 W. Only the windage and bearing losses take place in the prototype with a rotor without PMs in the generator idle mode. In the next step, the power consumption of the HSPMG drive with a rotor without PMs is measured. In this case, the power consumption of the drive motor is 320 W. The stator-core losses are than estimated at a high magnetization reversal frequency and the magnetic-flux density value below saturation. The power consumed by the drive motor is 324-325 W. Accordingly, the stator-core losses are 10 W/kg at a 2000 Hz frequency. These values correspond to the preliminary measurement data. The

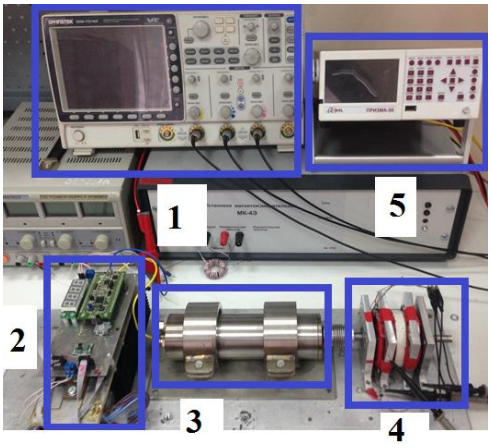

Figure 7. Test stand: 1 – oscillograph; 2 – an inverter with a 1000 Hz frequency; 3 – a drive motor; 4 – the HSPMG; 5 – a spectrum analyzer.

HSPMG workload is limited by the drive motor of the stand and does not exceed 1 kW. The *UI*-characteristic of the prototypes is measured using a variable resistance.

To assure the measurement accuracy of the eddy-current and hysteresis losses in the stator core, as well as the eddy-current losses in PM, the thermal state of all prototypes made of AMM and SiFe is also studied. A comparison of the core temperatures and losses and a comparison of the losses measured using the test bench and the HSPMG direct measurement are shown in Table 2. The losses in the AMM core are 137 % lower than in the FeSi core. A similar conclusion applies also for the temperature measurement: the AMM core temperature is 15 ºC lower. Thus, the experimental results confirm the theoretical assessment and effectiveness of the proposed technology and AMM in HSPMG. The losses obtained by the test bench are lower than those obtained by a direct measurement because the stator core is reversed by a sinusoidal magnetic field in the first case and a non-sinusoidal magnetic field in the direct measurement.

The steepness of the volt-ampere characteristic and overload capability coefficient k_e indicate the voltage reduction level under the current action, and the HSPMG overload capability. The smaller k_e the higher the HSPMG overload capability. This criterion is extremely important. The UAV generator must have a maximum overload capability. In an optimal topology, the volt-ampere characteristic must be less steep and k_e should be minimal. The requirements for the HSPMG overload capability are set by the MIL STD 704 standard. Fig. 8 shows the volt-ampere characteristic for

Table 2. Experimental results of losses at a 1000 Hz frequency and a 1.2 T magnetic-flux density.

Mate-rial	Loss, W test bench	Loss, W direct measurement	Tempe-rature, ºC
AMM	6.5	8.3	32
FeSi	17.7	19.7	47

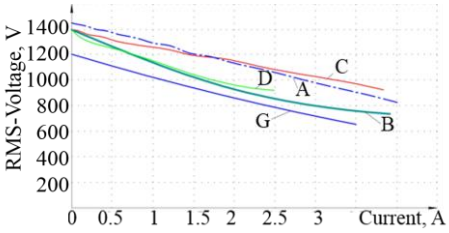

Figure 8. Volt-ampere characteristic of the studied topologies.

Table 3. Comparison of different HSPMG topologies

Topology	A	B	C	D	E
k_e	1.3	1.5	1.28	1.45	1.31
Total electrical losses, W	66	36.9	44	56.8	85.2
Power-to-mass ratio, kW/kg	4	3.57	4.55	4	5.26
Three-phase short-circuit current, A	19.8	20.8	21.9	22.3	21.2

each of the considered topologies. For the Type-F topology, it is not presented since it is of no particular interest. The Type-A and Type-E topology have a similar characteristic. Therefore, the volt-ampere characteristic of the Type-E topology is not given. It is important to notice that the volt-ampere characteristic of the Type-G topology is practically a straight line. This topology has less harmonic distortion than the topology with a tooth-coil winding and its overall dimension is similar to the Type-A and Type-E topology. Table 3 compares the topologies. The Type-A, Type-C and Type-E topology have the minimum k_e. The Type-B, Type-D, Type-F and Type-G topology have approximately the same k_e. Fig. 9 shows the back-EMF for each topology. The Type-D oscillogram has an asymmetrical character of the abscissa axis. The absence of the harmonic distortion in one part of the oscillogram increases the efficiency and reduces the HSPMG harmonic distortion. Moreover, a comparison between the experimental and simulation results shows that the discrepancy does not exceed 5 %. Thus, the simulation data are confirmed by the experimental data.

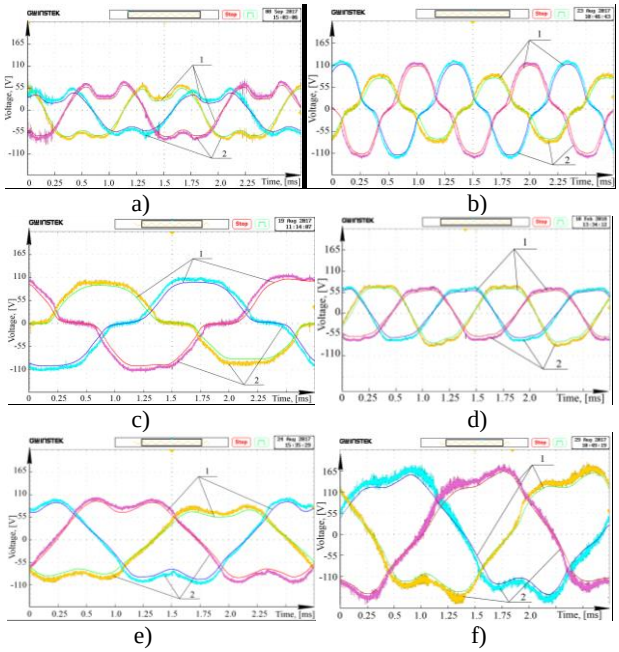

Figure 9. Back-EMF of the studied topologies: a) Type-A; b) Type-B; c) Type-C; d) Type-D; e) Type-F; f) Type-G; 1 – Simulation curve; 2 – Experimental curve

5 Conclusion

This paper compares different topologies of HSPMG with an AMM stator core. The results show that there is no unique optimal topology. The optimal topologies are the Type-C, Type-E and Type-F topology providing a minimal overall dimension and low losses. The Type-F topology has a maximum power-to-mass ratio, because each winding is located in a slot and does not intersect with the neighboring one. This result is achieved by using AMM. The losses in the AMM core are 137 % lower than in the FeSi core, and the AMM core temperature is 15 ºC lower. An HSPMG with a combined star delta winding is studied. This topology ensures low losses, but a low power-to-mass ratio. Using a combined winding reduces the PM eddy-current losses by 25 %. In general, it is recommended to use the Type-F topology (HSPMG with an AMM core) in UAV because of its efficiency and power-to-mass ratio.

Different HSPMG topologies with a six-slot AMM stator core using a 5-kW 60,000-rpm prototype are studied. The stator design is described and its effectiveness is experimentally proven. The manufacturing technology of the HSPMG stator core is described. Trends in the AMM core development and possible topologies are also studied.

Further research will be forwards designing a 60,000-rpm HSPMG with an AMM core and a power above 100 kW to be used in the aircraft auxiliary-power unit. Also, a commercial prototype of a 5 kW HSPMG is planned to be implemented and tested in UAV.

Acknowledgement

This work was supported by the Ministry of Education of the Russian Federation, project № 8.1277.2017/4.6.

References

[1] D. Gerada, A. Mebarki, N.L. Brown, C. Gerada, A. Cavagnino, A. Boglietti, High-Speed Electrical Machines: Technologies, Trends, and Developments, IEEE Transactions on Industrial Electronics, 61(6), pp. 2946–2959, 2014.

[2] N. Uzhegov, A. Smirnov, C.H. Park, J.H. Ahn, J. Heikkinen, J. Pyrhönen, Design Aspects of High-Speed Electrical Machines with Active Magnetic Bearings for Compressor Applications, IEEE Transactions on Industrial Electronics, 64(11), pp. 8427–8436, 2017.

[3] A. Borisavljevic, H. Polinder, J. Ferreira, On the Speed Limits of Permanent-Magnet Machines, IEEE Transactions on Industrial Electronics, 57(1), pp. 220–227, 2010.

[4] E. Ganev, Selecting the Best Electric Machines for Electrical Power Generation Systems, IEEE Electrification Magazine, 2(4), pp. 13–22, Dec. 2014.
[5] EnerTwin. [Online]. Available: http://www.hannovermesse.de/product/enertwin/2359397/L259910.
[6] J. Yun, S. Cho, H.C. Liu, H.-W. Lee, J. Lee, Design of electromagnetic field of permanent magnet generator for VTOL series-hybrid UAV, 2015 18th International Conference on Electrical Machines and Systems, pp. 83-86, 2015.
[7] N. Uzhegov, J. Pyrhönen, S. Shirinskii, Loss minimization in high-speed Permanent Magnet Synchronous Machines with tooth-coil windings, 39th Annual Conference of the IEEE Industrial Electronics Society, pp. 2960-2965, 2013.
[8] H. Zhang, X. Zhang, C. Gerada, D. Gerada, J. Li, Design considerations for the tooth shoe shape for high-speed permanent magnet generators, IEEE Transactions on Magnetics, 51(11), 2015.
[9] Y. Zhang, S. McLoone, W. Cao, Electromagnetic Loss Modeling and Demagnetization Analysis for High Speed Permanent Magnet Machine, IEEE Transactions on Magnetics, no. 99, pp. 1–5, 2017.
[10] F. Ismagilov, N. Uzhegov, V. Vavilov, V. Bekuzin, V. Ayguzina, Multidisciplinary Design of Ultra-High Speed Electric Machines, IEEE Transactions on Energy Conversion, 33(3), 8283793, pp. 1203-1212, 2018.
[11] N. Uzhegov, E. Kurvinen, J. Nerg, J. Pyrhönen, J.T. Sopanen, S. Shirinskii, Multidisciplinary Design Process of a 6-Slot 2-Pole High-Speed Permanent-Magnet Synchronous Machine, IEEE Transactions on Industrial Electronics, 63(2), pp. 784–795, 2016.
[12] A.J. Grobler, S.R. Holm, G. van Schoor, Empirical parameter identification for a hybrid thermal model of a high speed permanent magnet synchronous machine, IEEE Transactions on Industrial Electronics, 65(2), pp. 1616–1625, 2018.
[13] C. Zwyssig, J.W. Kolar, W. Thaler, M. Vohrer, Design of a 100 W, 500000 rpm permanent-magnet generator for mesoscale gas turbines, Conference Record of the 2005 Industry Applications Conference, pp. 253–260, 2005.
[14] C. Zwyssig, S.D. Round, J.W. Kolar, An ultra-high-speed, low power electrical drive system, IEEE Transactions on Industrial Electronics, 55(2), pp. 577–585, 2008.
[15] F. Ismagilov, V. Vavilov, D. Gusakov, N. Uzhegov, Topology Selection of the High-Speed High-Voltage PMSM for Aerospace Application, IECON 2017 - 43rd Annual Conference of the IEEE, 2017.
[16] Z. Wang et al., Development of an axial gap motor with amorphous metal cores, IEEE Transactions on Industry Applications, 47(3), pp. 1293–1299, 2011.
[17] S. Wu, R. Tang, W. Tong, X. Han, Analytical Model for Predicting Vibration Due to Magnetostriction in Axial Flux Permanent Magnet Machines With Amorphous Metal Cores, IEEE Transactions on Magnetics, 53(8), 2017.
[18] Radam Motors. [Online]. Available: http://www.radamllc.com/.
[19] R.L. Stoll, The Analysis of Eddy Currents. Oxford, England: Clarendon, 1974.
[20] SKF. Deep groove ball bearings. [Online]. Available: http://www.skf.com/group/products/bearings-units-housings/ball-bearings/deep-groove-ball-bearings/deep-groove-ball-bearings/index.html?designation=638%2F8-2Z.
[21] C. Huynh, L. Zheng, D. Acharya, Losses in High Speed Permanent Magnet Machines Used in Microturbine Applications, Journal of Engineering for Gas Turbines and Power, 131(2), pp. 1–6. 2009.

Flyur R. Ismagilov is a professor and head of the Department of Electromechanics of the Ufa State Aviation Technical University, Ufa, Russia. In 1973, he graduated from the Ufa Aviation Institute, Department of Electromechanics. In 1981 and 1998, he received his Ph.D. and D.-Sc. degrees in electrical engineering from the same university.

Jing Ou received his B.Sc. and M.Sc. degrees in electrical engineering from the Harbin Institute of Technology, Harbin, China, in 2011 and 2013, respectively. Since 2015, he has been working towards his Ph.D. degree in electrical engineering and information technologies at the Karlsruhe Institute of Technology, Karlsruhe, Germany. His research interests include design and control of electrical machines.

Viacheslav Ye. Vavilov is an associate professor at the Department of Electromechanics of the Ufa State Aviation Technical University, Ufa, Russia.
He received his specialist and Ph.D. degrees in electrical engineering from the same university in 2010 and 2013, respectively.

Denis V. Gusakov is a senior lecturer at the Department of Electromechanics of the Ufa State Aviation Technical University, Ufa, Russia.
He received his specialist and Ph.D. degrees in electrical engineering from the same university in 2011 and 2016, respectively.

Valentina V. Ayguzina is a postgraduate student at the Department of Electromechanics of the Ufa State Aviation Technical University, Ufa, Russia, where she graduated from in 2016.

Aleksey M. Veselov is a postgraduate student at the Department of Electromechanics of the Ufa State Aviation Technical University, Ufa, Russia, where he graduated from in 2017.